Journal of Achievements in Materials and Manufacturing Engineering
VOLUME 61
ISSUE 2
December
2013

Control of optical active borates nanocrystals agglomeration

I. Cieślik [a,*], R. Węgłowski [b], J. Żmija [b], K. Kurzydłowski [c], M. Płocińska [c], M. Oćwieja [d]

[a] Material Physics Department, National Center for Nuclear Research, ul. A. Sołtana 7, 05-400 Otwock, Poland
[b] Institute of Optoelectronics, Military University of Technology, ul. S. Kaliskiego 2, 00-908 Warszawa, Poland
[c] Faculty of Materials Science and Engineering, Warsaw University of Technology ul. Wołoska 141, 02-507 Warszawa, Poland
[d] Institute of Catalysis and Surface Chemistry Polish Academy of Sciences ul. Niezapominajek 8, 30-239 Kraków, Poland
* Corresponding e-mail address: icieslik@wat.edu.pl

Received 13.10.2013; published in revised form 01.12.2013

Materials

ABSTRACT

Purpose: The purposes of this study explore the possibility of total control the agglomeration of nanoborates powders. The great potential of PDLCs can be enhanced by using dye-doped or nanoparticles-doped materials, such as borates [1]. It is important to know how to prepare nanoparticles in order to obtain a high level of dispersion in the composites. Otherwise, even small an agglomeration does not give a possibility on the appropriate characteristic of properties and interpretation of the results. The deagglomeration methods applied until now give the decrease of agglomeration to a lesser extent than our method. Characteristic size and shape of particles made with sol-gel process is difficult to perform.
Design/methodology/approach: Nanopowders samples of YAB and LCBO were prepared with sol-gel method. Deagglomeration process was carried out using acetic acid. The morphology and size of nanopowders were investigated by scanning electron microscopy (SEM). The crystallite sizes were determinated with IPS UA method.
Findings: It was confirmed that the acetic acid influence on the decrease of agglomeration. It was also determined of conditions for preparation borates nanopowders samples (concentration acetic acind time and temperature of drying prepared samples). We have proved that a reagent used for deagglomeration process does not affect the structure of the investigated nanoborates used in an experimental.
Research limitations/implications: The results can be used to the prepared of nanocompades of borates to observe a morphology and reliable assessment of nanocrystalline size.
Originality/value: Our study shows how to prepare a sample of particles to observe morphology and measure the size of nanograins. In our study we found excellent solution, the medium, which not influence the inorganic nanomaterial structure. Result seems to be excellent and very perspective. We have showed as that measurement type influence the results of particles size.
Keywords: Nanocrystals; Borates; Agglomeration; Nonlinear properties; Composites

Reference to this paper should be given in the following way:
I. Cieślik, R. Węgłowski, J. Żmija, K. Kurzydłowski, M. Płocińska, M. Oćwieja, Control of optical active borates nanocrystals agglomeration, Journal of Achievements in Materials and Manufacturing Engineering 61/2 (2013) 163-168.

1. Introduction

The conventional sol-gel process has been known since the late 18th century [2]. This method represents an attractive approach for producing nanomaterials. Otherwise, the sol-gel technique is widely used for the preparation of ceramics, glasses, thin films, fibers, nanocompounds and compositematerials. Furthermore, with the use of the sol-gel process various homogenous and pure materials can be formed at a low temperature.

The principal drawback of this method is agglomeration of the final products [3]. Wang et al. reported that sintering of powders opens the way to a higher sintered density [4]. Thus, the last stage of the process is affected by the agglomeration of the particles. A greater agglomeration effect is expected at higher sintering temperatures. The temperature depends on the type of the components used. In the literature it can be found that problematic gel impurities, such as: NO_3^- and HO^- led to the solid bridging carbonization process [5]. In the same paper Bangyao et al. showed that the addition of some organic components to the initial gel led to the elimination of agglomerates in the complexing sol-gel method.

However, the last steps of these processes, where nanopowders are sintered and purified, considerably increase the agglomeration rate and particles size. The grain size studies also become challenging.

Contrary to the abovementioned research results we have shown that ethylene glycol is effective only in controlling the particles size during the sol-gel process [6]. Otherwise, ethylene glycol allows for obtaining micrometer grain size only in the case of using the polymeric sol-gel method. It has been indicated that suspending inorganic nanoparticles in polymer leads to a reduction in the undesirable agglomeration effect.

In the recently years hard ceramic particles start to be used for reinforcement or giving new, properties to several types of composites [7,8] including Polymeric Dispersed Liquid Crystals (PDLC) [9].

The phenomenon of agglomeration persisted in PDLC composites doped with inorganic nanoparticles in humid conditions. A major role starts to be played by capillary forces that increase the particles adhesion [10]. The agglomeration of nanoparticles does not enable a proper dispersion in the composites.

In our research we obtained nanoborate materials, such as: yttrium aluminum borate (YAB) and calcium lanthanum borate (LCBO). Due to nonlinear optical properties of inorganic nanocrystals they can be used for the production of electro-optical composite materials like PDLC systems [9]. YAB is material with space group R32 and is excellent host for RE active ions. This allows to develop self-frequency doubling and self-frequency-sum solid state lasers [11,12]. LCBO is material with space group C2 and exhibits a relatively large optical second-harmonic generation effect [13-15].For many years these borates materials were obtained in single crystals form by means first of all Czochralski method or High Temperature Solution Growth (flux method) [16]. Last year's gave possibilities to obtain these materials in form of powder. Because of this new possibilities of applications of composites with excellent electro-optical properties were introduced. Nanopowders can be fabricated using powder metallurgy process, which is relatively easy to control [17]. However, in this case powder metallurgy seems to be more expensive and does not give a possibility to obtained high purity products. Therefore, in order to optimize the optical properties of these materials a uniform distribution of nanoparticles within the whole volume must be provided. Controlling nanoparticles agglomeration in dry powder is essential.

2. Experimental

2.1. Materials

Analytically pure $YAl_3(BO_3)_4$, $La_2CaB_{10}O_{19}$, CH_3COOH, HCl, NaCl, NaOH, were used (Sigma Aldrich). The other chemical compounds were of analytical purity as well.

2.2. Nanopowders samples preparation

Samples of yttrium aluminum borates or lanthanum calcium borates nanocrystals were put into acetic acid or hydrochloric acid solution to obtain acidic environment. Sodium hydroxide was used to obtain the basic range of pH. The pH of the studied suspensions ranged from 0.3 to 13.4. In the next step the samples were subjected to ultrasonic cleaning (at 32 [W]) for 4 or 8 hours each sample. After that droplets of the solutions were placed on glass plates. The prepared plates were dried at 120°C for 5 hours to remove water. To investigate the nanopowders agglomeration rate of inorganic compounds we used scanning electron microscopy (SEM SU 8000 Hitachi). For the imaging magnification ranges of 50,000 to 130,000 times were used.

2.3. The zeta potentiale

The average crystallite sizes and agglomeration rate were determined with the Sherrer method, SEM technique and laser diffractometry.

The particle size distribution was determined by laser diffractometry using the Beckman-Coulter Laser Diffraction Particle Size Analyzer LS 13 320. The zeta potential of the particles was determined by microelectrophoresis by means of a Zeta Pals Broohaven Instrument. Using a unique technique (Laser Doppler Velocimetry) Zeta Pals Broohaven Analyzer we measured the microelectrophoretic mobilities of charged nanoparticles in the wide size range of 5 nm to 50 nm. In this method, voltage was applied across a pair of electrodes placed at the both ends of a cell containing the particle sol. Charged nanoparticles were moved to an oppositely charged electrode, and their velocity was measured and expressed as electrophoretic mobility.

The zeta potentials of particles were calculated using the following equation (Henry's formula):

$$\zeta = \frac{3\eta}{2\varepsilon f(\kappa a_p)} \mu_e \quad (1)$$

where: ζ - the zeta potential of the particles, ε - the dielectric permittivity of water, μ_e- the electrophoretic mobility of colloidal particles, $f(\kappa a_p)$ - a function of the dimensionless parameter κa_p, where κ^{-1} is the thickness of the electric double-layer:

$$\kappa^{-1} = \left(\frac{\varepsilon kT}{2e^2 I}\right)^{\frac{1}{2}} \quad (2)$$

where: e is the elementary charge, I is the ionic strength:

$$I = \frac{1}{2}\sum_i c_i z_i^2 \quad (3)$$

where: c_i - the ion concentration, and a_p is the particle radius. The zeta potentials of particles were determined for an ionic strength of $I=10^{-2}$ M (regulated by NaCl addition) and a pH range was from 2 to 12 using Smoluchowski approximation.

3. Results and discussion

3.1. Zeta potential measurement

Figs. 1a and 1b show the zeta potential dependent features of YAB and LCBO, nanopowders ζ [mV] on the pH value. The pH value varied during the measurements from 2 to 12. The zeta potential value for nanopowders of YAB falls on pH=8.2 (Fig. 1a). When the value of pH is at an isoelectric point, the most agglomerated nanometric size YAB particles can be observed. The positive and negative charges were dominated on the surface of powders connected to attract the particles into big agglomerates.

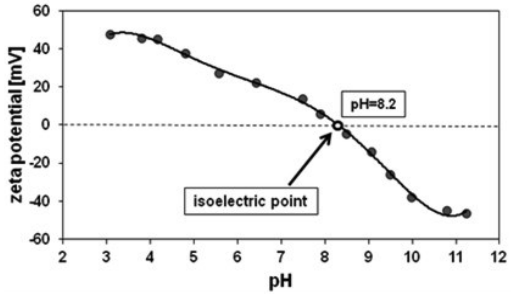

Fig. 1a. Dependence of the zeta potential on the pH values at room temperature for YAB nanopowder. The measurements were performed for 500 ppm of YAB concentration and an ionic strength of I = 10^{-2} M NaCl

A similar phenomenon was observed for LCBO nanopowder in Fig. 1b (at pH=8.8). Thus, for both samples pH ranges of pH=2-3 and pH=11-12 is appropriate to reduce the agglomerated YAB and LCBO particles.

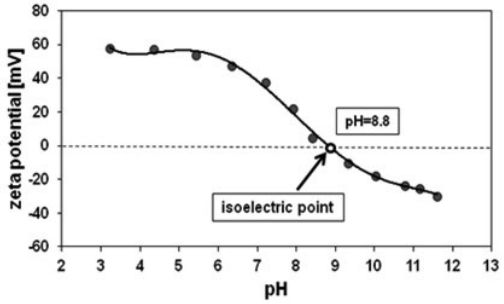

Fig. 1b. Dependence of the zeta potential on the pH values at room temperature of LCBO nanopowder. The measurements were performed for 500 ppm of LCBO concentration and an ionic strength of I = 10^{-2} M NaCl

3.2. The affect of ultrasounds on deagglomeration of inorganic nanopowders

As shown in the pictures (Figs. 2 and 3), nanoparticles treated with ultrasounds are deagglomerated as opposed to particles not subjected to ultrasound treatment. The ability to deagglomerate after being treated with ultrasound for 8 hours is better than for 4 hours for nanoparticles of YAB (Figs. 2b and 2c) and LCBO (Figs 3b and 3c). In fact, using ultrasound treatment without applying the appropriate pH is not sufficient to achieve strong deagglomeration of nanoparticles. As it can be seen, nanoparticles deagglomeration rate is the best for 8 hours of ultrasonication.

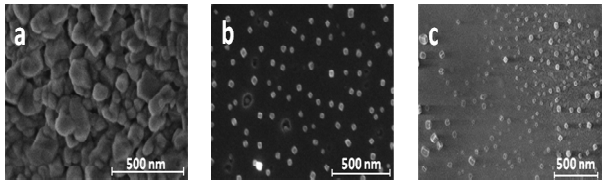

Fig. 2. Scanning electron microscopy (SEM) images of nanopowder of $YAl_3(BO_3)_4$ with and without ultrasound treatment at pH = 0.3 Duration of ultrasonic treatment: a) t=0 h, b) t=4 h, c) t=8 h

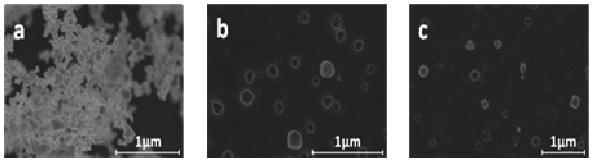

Fig. 3. SEM images of nanopowder of LCBO with and without ultrasound at the same pH=1.8. Duration of ultrasonic treatment: a) t=0 h, b) t=4 h, c) t=8 h

3.3. The effect of pH on nanopowders deagglomeration

Figs. 4 and 5 present changes in agglomeration of inorganic nanopowders dependent on the pH of the environment. During our studies the pH value of the environment ranged from 0.3 to 13.4 causing a substantial difference in the degree of deagglomeration. In order to obtain the maximum deagglomeration of yttrium aluminum borates powder a low pH is needed (Fig. 4a). With the use a higher pH = 13.4 significant agglomeration can be observed (Fig. 4c). Nevertheless, the results of a comparative study of agglomeration between samples of YAB powders in basic environment (Fig. 4a) and YAB powders in neutral environment (Fig. 4b) are meaningful. In case of the others inorganic nanopowders lanthanum calcium borates (LCBO) a similar conclusion can be drawn. Fig. 5 shows examples of agglomeration of the LCBO particles obtained at three different pH values. Effective deagglomaration of LCBO particles was observed at pH=1.8, as can be seen in Fig. 5a.

Figs. 5b and 5c show LCBO powder at a neutral and at a basic pH. Unfortunately, the strongly bound agglomerates of particles were not reduced. Thanks to the particles size measurements using SEM images the analysis of samples YAB and LCBO in acidic pH range was possible.

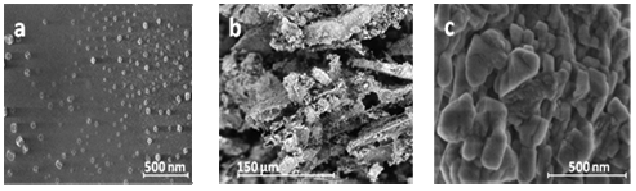

Fig. 4. SEM images of YAB nanopowders ultrasonicated for 8 hours at different pH values: a) pH=0.3 t=8, b) pH=0, c) pH=13.4

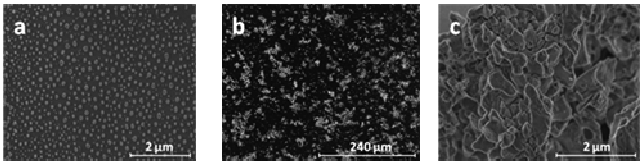

Fig. 5. SEM images of LCBO nanopowder ultrasonicated for 8 hours at different pH values: a) pH=1.8, b) pH=0, c) pH=13.4

3.4. The effect of the medium on nanopowders deagglomeration

The analysis of acetic acid was performed by spectrometer IR using Nicolet iS10 Thermo Scientific. Fig. 6 shows IR spectra of acetic acid and acetic acid with suspended nanopowders of YAB and LCBO. There is a stretched peak of O-H (3700÷2800 cm^{-1}), also including C-H 3000÷2800 cm^{-1}, a narrow peak of CO_2 (2360 cm^{-1}), band peak of H-O (1635 cm^{-1}), band peak of C=O (1394 cm^{-1}) and a stretched peak of C-H (1278 cm^{-1}) in organic acid without nanopowders.

These peaks almost completely overlap with spectrum of nanopowders of YAB and LCBO in acetic acid. However, intensity of peaks is a little smaller.

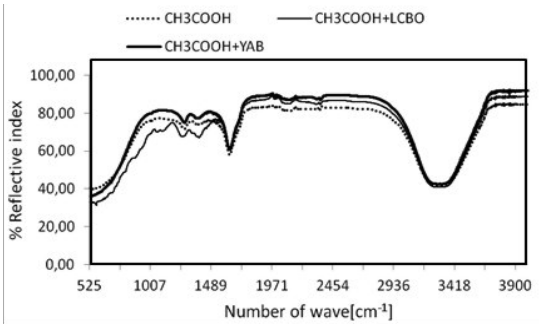

Fig. 6. IR spectra of the CH_3COOH a) without nanopowders b) with nanopowders of $YAl_3(BO_3)_4$, c) with nanopowders of $La_2CaB_{10}O_{19}$

3.5. The nanocrystals size before deagglomeration (IPS UA method)

The distribution of particles size of borates ($YAl_3(BO_3)_4$, $La_2CaB_{10}O_{19}$,) was measured. An analysis of particles size distribution of borates powders before the deagglomeration process was performed using the aerodynamic aerosol analyzer method (UVAPS 3314). The results are shown in Figs. 7 and 8. The maximum particles size depends on the kind of borates powders. Fig. 7 shows the distribution of particles size of $YAl_3(BO_3)_4$ with a maximum at about 3.5 µm. Fig. 8 shows a maximum at about 6 µm. Distribution of YAB particles size (Fig. 7) is much narrower than that for the other borates powders (Fig. 8). In Fig. 8 is a broad distribution of particles size is presented. The particles size reached a value of about 45 µm.

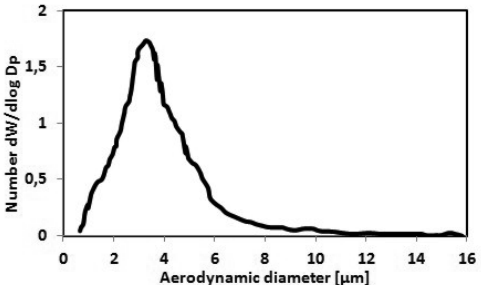

Fig. 7. Histogram of the distribution of YAB particles size before deagglomeration

3.6. The nanocrystals size after deagglomeration

In order to perform a comparison with the previous results the grain size distribution of borates ($YAl_3(BO_3)_4$, $La_2CaB_{10}O_{19}$,)

particles after deagglomeration process–was measured. We used SEM imaging to measure the particles size of powders after deagglomeration. Fig. 9 shows SEM photographs of YAB nanopowders after deagglomeration. The agglomerates of nanoparticles were completely reduced to primary particles. A similar phenomenon was observed for other borates powders shown in Fig. 10.

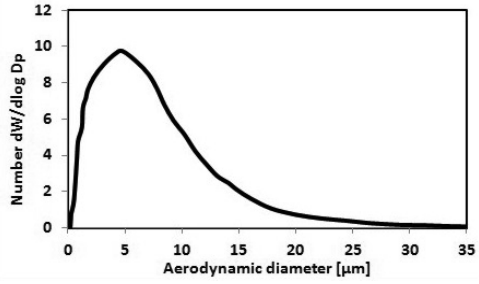

Fig. 8. Histogram of the distribution of LCBO particles size before deagglomeration

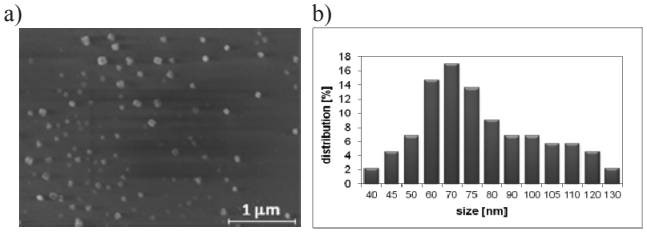

Fig. 9. Distribution of nanocrystalline size of YAB powder after deagglomeration: a) SEM image, b) histogram showing results of Image Pro Plus 5.0 analysis

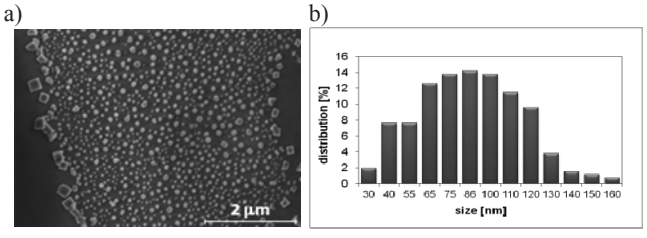

Fig. 10. Distribution of nanocrystalline size of LCBO powder after deagglomeration: a) SEM image, b) histogram showing results of Image Pro Plus 5.0 analysis

3.7. The measurement errors for the nanocrystals size

Figs. 11 and 12 show the result of a comparison between nanocrystals size measurement before and after deagglomeration test. The difference is immense for both samples of YAB and LCBO nanocrystals. Hovewer, the difference for samples of LCBO powder is twice greater than for samples YAB of powder.

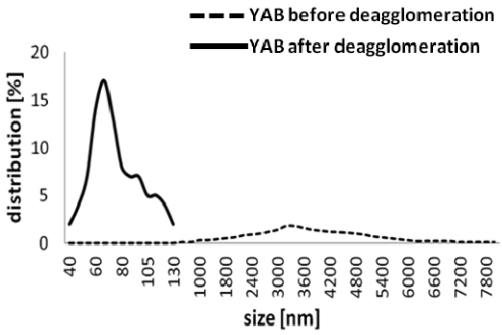

Fig. 11. The distribution of the particles size of YAB before and after deagglomeration calculated from SEM images

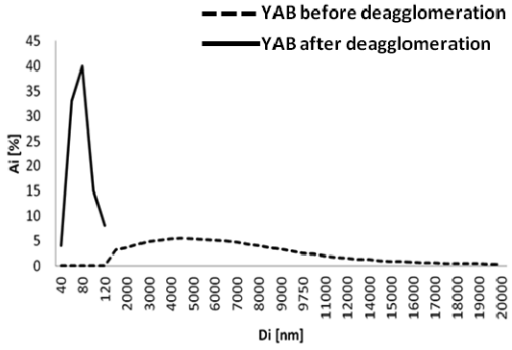

Fig. 12. The distribution of the particles size of LCBO before and after deagglomeration calculated from SEM images

4. Conclusions

We have studied the deagglomeration of inorganic nanopowders samples of (YAB) and (LCBO) obtained using the sol-gel method. Acetic acid and sodium hydroxide as dispersing media were used to reduce agglomeration problems through surface modification of particles. The influence of the pH value on inorganic nanopowders has been discussed. In the presented method powders deagglomeration was achieved by changing the pH of the inorganic nanoparticles suspension. The pH value is individual for each of the inorganic nanoparticles and depends on the type of atoms in the structure, the type of synthesis and the solvents used. In our research a solution of acetic acid was a sufficient medium for deagglomeration of YAB and LCBO agglomerated powders. The degree of agglomeration was reduced due to the repulsion of the charged particles.

We have proved that a reagent used for deagglomeration process (acetic acid) does not affect the structure of the investigated nanopowders. We have demonstrated a high influence of agglomeration of nanopowders on the particles size measurements, which causes the errors. At the next stage of our research we are willing to obtain a proper dispersion of nanoparticles in the whole volume of the PDLC composite.

Acknowledgements

This work was financed partially from the PBS Project No 23-848.

References

[1] K.B. Zegadlo, H.E. Ouazzani, I. Cieślik, R. Węgłowski, J. Żmija, S. Kłosowicz, A. Majchrowski, J. Myśliwiec, B. Sahraoui, M. Karpierz, Nonlinear optical properties of polymer dispersed liquid crystals doped with $La_2CaB_{10}0_{19}$, Optical Materials 34 (2012) 1704-170.

[2] Y. Dimitriev, Y. Ivanowa, R. Iordanowa, History of sol- gel science and technology, Journal University Chemical Technology Metallurgy 43/2 (2008) 181-192

[3] S. Li, B. Bergman, Z. Zhao, Synthesis and characterization of lanthanum aluminate powders via a polymer complexing plus combustion route, Materials Chemistry and Physics 132 (2012) 309-315.

[4] C.T. Wang, L.S. Lin, S.J. Yang, Preparation of $MgAl_2O_4$ Spinel Powders via Freeze-Drying of Alkoxide Precursors, Journal of the American Ceramic Society 75/8 (1992) 2240-2243.

[5] Y. Bangyao, W. Lingsen, F. Yi, Z. Jinsheng, Agglomerate control in complexing sol-gel process, Transactions of Nonferrous Metal Society in China 9/4 (1999) 712-716.

[6] I. Cieślik, J Żmija, A. Majchrowski, M. Pępczyńska, P. Morawiak, M. Włodarski, Synthesis and characteristic of optical properties of crystalline $YAl_3(BO_3)_4$: Cr, Ce, Journal Achievers Materials and Manuacturing Engineering 48 (2011) 24-28.

[7] A. Włodarczyk-Fligier, L.A. Dobrzański, M. Adamiak, Wear resistance of PM composite materials reinforced with the Ti(C,N) ceramic particles, Journal of Achievements in Materials and Manufacturing Engineering 30/2 (2008) 147-150.

[8] A. Włodarczyk-Fligier, L.A. Dobrzański, M. Adamiak, Corrosion resistance of the sintered composite materials with the EN AW-AlCu4Mg1 alloy matrix reinforced with ceramic particles, Journal of Achievements in Materials and Manufacturing Engineering 42/1 (2010) 120-127.

[9] R. Węgłowski, S.J. Kłosowicz, A. Majchrowski, S. Tkaczyk, A.H. Reshak , J. Pisarek, I.V. Kityk, Enhancement of the Kerr response in polimer-dispersed liquid crystal complexes due to incorporation of BiB_3O_6 nanocrystallites, Mateials Letter 64 (2010) 1176-1178.

[10] J.A. Kurkela, D.P. Brown, J. Raula, E.I. Kauppinen, New apparatus for studying powder deagglomeration, Powder Technology 180 (2008) 164-171.

[11] G. Dominiak-Dzik, W. Ryba-Rymanowski, M. Grinberg, E. Beregi, L. Kovacs, Excited state relaxation dynamice of Cr 3+ in $YAl_3(BO_3)_4$, Journal of Physics Condensed Matter 14 (2002) 5229-5237.

[12] E. Cavalli, A. Speghini, M. Bettinelli, M.O. Ramirez, J.J. Romeo, L.E. Bausa, J. Garrcia Sole, Luminescence of trivalent rare earth ions in the yttrium aluminum borate non-linear laser crystal, Journal of Luminescence 102-103 (2003) 216-219.

[13] J. Wang. P. Fu, Y. Wu, Top - seeded growth and morphology of $La_2CaB_{10}O_{19}$ crystals, Journal of crystal growth 235 (2002) 5-7.

[14] Y.Wu, P.Fu, X. Guan, C. Chen, G. Wang, J. Lu, Z. Xu, Optical characterization of a new lanthanum and calcium borate La/sub 2/CaB/sub 10/O/sub 19/, Laser and Electro-Optics 2 (2001) 11-12.

[15] R. Arun Kumar, Borate Crystals for Nonlinear Optical and Laser Applications: A Review, Journal of Chemistry 2013 (2013) 154862.

[16] A. Majchrowski, T. Łukasiewicz, Z. Mieczyk, M. Malinowski, Optical properties of some borate single crystals, Growth, Characterization, and Applications of Single Crystals 4412 (2001) 74-82.

[17] A. Włodarczyk-Fligier, L.A. Dobrzański, M. Kremzer, M. Adamiak, Manufacturing of aluminum matrix composite materials reinforced by Al_2O_3 particles, Journal of Achievements in Materials and Manufacturing Engineering 27/1 (2008) 99-102.